

Electric Dipole Echoes in Rydberg Atoms

S. Yoshida,¹ C. O. Reinhold,^{2,3} J. Burgdörfer,^{1,3} W. Zhao,⁴ J. J. Mestayer,⁴ J. C. Lancaster,⁴ and F. B. Dunning⁴

¹*Institute for Theoretical Physics, Vienna University of Technology, Vienna, Austria, EU*

²*Physics Division, Oak Ridge National Laboratory, Oak Ridge, Tennessee 37831-6372, USA*

³*Department of Physics, University of Tennessee, Knoxville, Tennessee 37996, USA*

⁴*Department of Physics and Astronomy and the Rice Quantum Institute, Rice University, Houston, Texas 77005-1892, USA*

(Received 14 February 2007; published 15 May 2007)

We report the first observation of echoes in the electric dipole moment of an ensemble of Rydberg atoms precessing in an external electric field F . Rapid reversal of the field direction is shown to play a role similar to that of a π pulse in NMR in rephasing a dephased ensemble of electric dipoles resulting in the buildup of an echo. The mechanisms responsible for this are discussed with the aid of classical trajectory Monte Carlo simulations.

DOI: [10.1103/PhysRevLett.98.203004](https://doi.org/10.1103/PhysRevLett.98.203004)

PACS numbers: 32.80.Rm, 32.80.Qk, 76.60.Lz

The average magnetization of an ensemble of nuclear magnetic dipole moments precessing about a static magnetic field is attenuated due to variations in the local magnetic fields and the resulting precession velocities ω . By applying an alternating magnetic field pulse (typically a $\pi/2$ or π pulse) transverse to the static field after a time τ , this attenuation by dephasing can be reversed resulting in the reappearance, after $t = 2\tau$, of a significant fraction of the initial magnetization, the “echo” of the original signal. This “spin echo” was discovered by Hahn [1] over 50 years ago. The remarkable observation in nuclear magnetic resonance (NMR) [2] of a laboratory “time-reversal operation” for a statistical ensemble of quantum systems touches on many ideas related to nonequilibrium statistical mechanics (reversal of the “arrow of time”), the interplay between dephasing and decoherence [3], classical-quantum correspondence, and coherent control and manipulation of quantum systems [4]. Other echo phenomena including photon echoes [5,6] where single-photon wave packets are intermittently “stored” in the wave function of a coherently excited few-level atom to be retrieved later as an echo have been observed. The Loschmidt echo [7] probes the influence of classical chaos on quantum wave packets. Small changes in the Hamiltonian between the forward and backward propagation times $0 < t < \tau$ and $\tau < t < 2\tau$, respectively, lead to an exponential suppression of echoes when the underlying classical dynamics is chaotic.

We report here the observation of echoes in the electric dipole moment of an ensemble of free Rydberg atoms. Manipulation of Rydberg states with large principal quantum numbers n is of considerable interest for implementation of fast quantum gates [8], for quantum information registers [9], and for the dipole blockade [10], which inhibits transitions to all but singly excited collective states. More generally, high- n Rydberg atoms provide a valuable mesoscopic laboratory to explore concepts and technologies for quantum information processing and coherent control [11,12]. While the precession of an electric dipole moment has many features in common with its

magnetic counterpart, realization of an echo in the electronic motion of atoms provides additional challenges because of the shorter time scale for orbital and precessional motion and the much stronger coupling of such microsystems to their environment leading to rapid decoherence [13] or even destruction.

The present protocol employs $n \sim 350$ Stark wave packets with binding energies $E = -1/(2n^2)$ in the sub-meV regime and electron orbital periods $T_n = 2\pi n^3$ of a few nanoseconds (we use atomic units unless otherwise stated). Echoes are generated by rapidly reversing the electric field about which the dipole moments precess. Phase coherence in low- n wave packets has been explored earlier using revivals [14] but this is not possible at high- n because typical revival times exceed the decoherence time τ_D . Dipole echoes, however, can be observed on much shorter time scales, allowing study of the onset of decoherence.

For a given n level electron motion in a weak electric field $\vec{F} = F\hat{z}$ can be discussed with the aid of the pseudospins $\vec{J}_\pm = (\langle \vec{L} \rangle \pm n\langle \vec{A} \rangle)/2$, where $\vec{L} = \vec{r} \times \vec{p}$ and $\vec{A} = \vec{p} \times \vec{L} - \hat{r}$ are the angular momentum and the Runge-Lenz vector, respectively [15]. To first order in F , the time evolution of the pseudospins obeys two decoupled effective Bloch equations [16]

$$\frac{d}{dt} \vec{J}_\pm = \omega_\pm(F) \vec{J}_\pm \times \hat{z}. \quad (1)$$

The pseudospins precess in opposite directions about the field with angular velocities $\omega_\pm \approx \pm(3/2)Fn (\equiv \omega_\pm^{(1)})$ (Fig. 1) much like spin precession in a magnetic field. However, the electric dipole (proportional to \vec{A}) changes periodically in time. The magnitudes of $\langle \vec{L} \rangle = \vec{J}_+ + \vec{J}_-$ and $n\langle \vec{A} \rangle = \vec{J}_+ - \vec{J}_-$ take on maximal (and minimal) values twice during one precession orbit and oscillate with the Stark frequency $\omega_s = 2\omega_+^{(1)}$ corresponding to the hydrogenic Stark splitting within the n manifold. Equation (1) holds both quantum mechanically and classically and is identical to the equation governing the motion of a single spin magnetic moment in NMR. A Rydberg wave packet

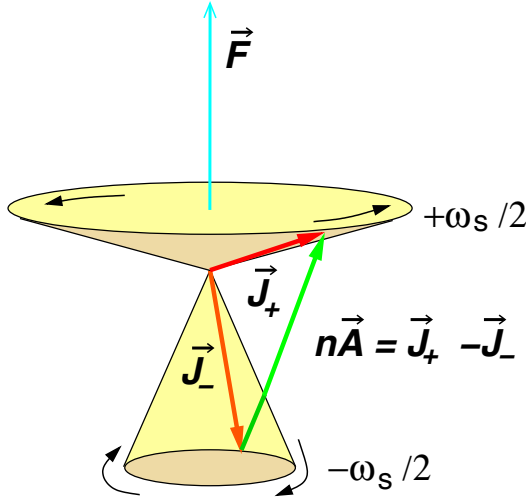


FIG. 1 (color online). Behavior of the pseudospins \vec{J}_{\pm} . To first-order these precess with angular velocities $\pm\omega_s/2$ in the electric field. The electric dipole is proportional to $n\langle\hat{A}\rangle = (\vec{J}_+ - \vec{J}_-)$.

containing components with different values of n possesses a broad range of precession frequencies $\omega_s(n)$, corresponding to the inhomogeneous line broadening observed for an ensemble of spins in NMR, leading to the dephasing of the wave packet.

In the experimentally available parameter range, the dynamics of the electric dipole is more complex due to couplings to internal degrees of freedom in the atom causing dephasing of wave packets even within an n manifold. A typical Rydberg electron trajectory [Figs. 2(a) and 2(b)] embodies three different time scales. The electron orbits rapidly on an approximate Kepler ellipse with period T_n . This ellipse precesses in the field and undergoes oscillations in eccentricity on an intermediate time scale $T_k \sim 2T_s = 4\pi/\omega_s$ [Fig. 2(a)]. Such Stark precession results in an elliptic trajectory of the Runge-Lenz vector in the $(A_x,$

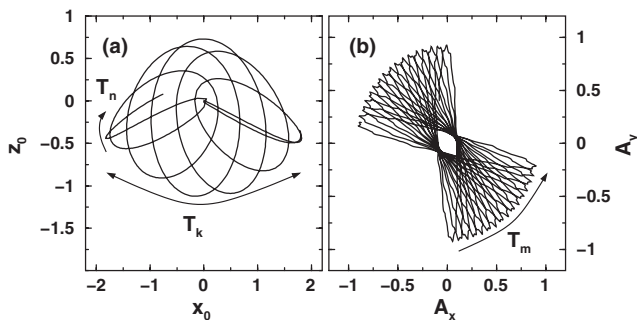


FIG. 2. Time evolution of the classical trajectory of a single Rydberg electron ($n = 350$) in an external electric field $F = 20$ mV/cm applied along the z direction: (a) projection of the trajectory onto the (z, x) plane during a Stark precession period ($T_s \approx T_k/2 \approx 40$ ns) equal to about seven Kepler periods ($T_n = 6.5$ ns). (b) Slow rotational motion in the (A_x, A_y) plane for $0 \leq t \leq 1000$ ns ($T_m \approx 2500$ ns). All coordinates are depicted in scaled units ($r_0 = r/n^2$, $p_0 = pn$).

$A_y)$ plane [Fig. 2(b)]. This ellipse slowly rotates about the A_z axis with period T_m . These three time scales can be derived from the eigenenergies given by second-order hydrogenic quantum perturbation theory

$$E_{n,k,m} = -\frac{1}{2n^2} + \frac{3}{2}nkF - \frac{1}{16}F^2n^4[17n^2 - 3k^2 - 9m^2 + 19], \quad (2)$$

where k and m are the electric and magnetic quantum numbers, respectively. Remarkably, Eq. (2) agrees with the classical result [17] in terms of the actions n , k , and m up to small corrections due to noncommutativity. Expressing the classical energy in terms of the z components of the pseudospins, $J_{\pm}^z = (m \pm k)/2$, the precession frequencies in Eq. (1) are

$$\begin{aligned} \omega_{\pm}(F) &= \frac{\partial E(n, J_{\pm}^z, J_{\pm}^z)}{\partial J_{\pm}^z} \\ &= \pm[\omega_k^{(1)}(F) + \omega_k^{(2)}(F)] + \omega_m^{(2)}(F), \end{aligned} \quad (3)$$

where $\omega_k^{(1)} = 3Fn/2$ is the first-order angular velocity, and $\omega_k^{(2)}(F) = (3/8)F^2n^4k$ and $\omega_m^{(2)}(F) = (9/8)F^2n^4m$ are the second-order corrections proportional to the electric

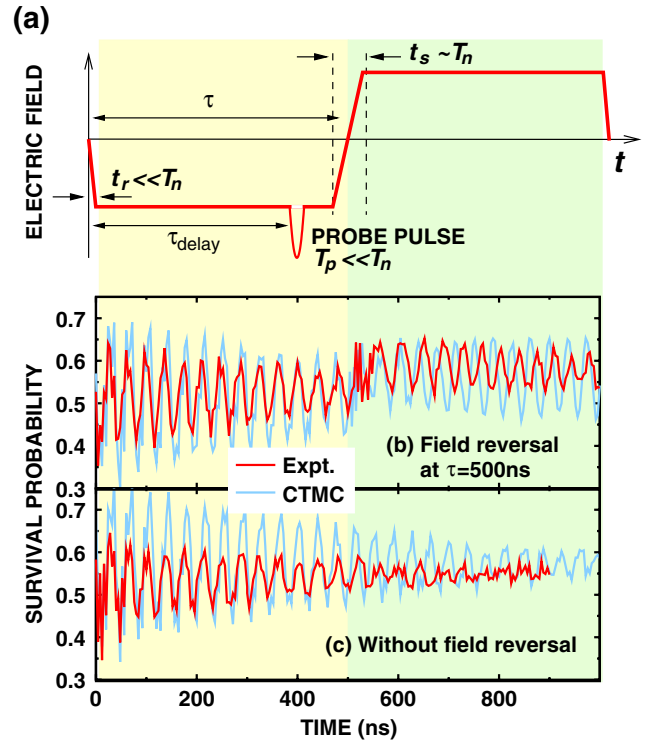


FIG. 3 (color online). (a) Time-dependent field used to study the dipole echo (see text). The probe HCP, with scaled amplitude $n\Delta p_p = 0.53$, is applied after a variable delay time. (b) Echo in the time-resolved survival probability (experiment: red, CTMC simulation: blue) for $n = 350$ atoms initially polarized along the x axis and a field $|F| = 20$ mV/cm applied in the z direction. The field is reversed at $\tau = 500$ ns. (c) Time-resolved survival probability without field reversal.

(k) and magnetic (m) quantum numbers. The Kepler frequency $\omega_n = \partial E(n, J_+^z, J_-^z)/\partial n = 2\pi/T_n$. The angular velocity $\omega_m^{(2)}$, which determines the rotation period, $T_m = 2\pi/\omega_m^{(2)}(F)$, in the (A_x, A_y) plane [Fig. 2(b)] is identical for both pseudospins. (Note that the second-order correction lifts the degeneracy between the magnitude of the frequencies ω_+ and ω_- .) It can be separated from the Stark precession by transforming the pseudospins into a rotating frame, $\vec{J}'_{\pm} = R_z(\phi = \omega_m t)\vec{J}_{\pm}$, where $R_z(\phi)$ is the matrix for rotation by an angle ϕ about the z axis. To second order in F , the Bloch equations in the rotating frame become

$$\frac{d}{dt}\vec{J}'_{\pm} = \pm\omega_k(F)\vec{J}'_{\pm} \times \hat{z} \quad (4)$$

with $\omega_k(F) = \omega_k^{(1)}(F) + \omega_k^{(2)}(F)$ [i.e., a precession period $T_k = 2\pi/\omega_k(F)$]. A wave packet has a distribution of actions (quantum numbers) n and k which translate into n and J_{\pm}^z , and is interpreted as an ensemble of spins with a broad distribution of $\omega_k(F)$.

To investigate Stark echoes experimentally, quasi-one-dimensional Rydberg atoms oriented along the x axis are first produced by photoexciting potassium atoms to a mix of the lowest-lying redshifted states in the $n = 350$ Stark manifold in a weak ($\sim 250 \mu\text{V cm}^{-1}$) dc field (directed along the x axis) [18]. A much larger dc field $F = 20 \text{ mV cm}^{-1}$ is then suddenly applied (rise time $\sim 0.3 \text{ ns} \ll T_n$) in the z direction [Fig. 3(a)] to create a Stark wave packet comprising a coherent superposition of Stark states with a narrow range of n . The wave packet is allowed to evolve in the field for a time $\tau = 500 \text{ ns}$ whereupon the field is reversed $F \rightarrow -F$. The switching time $t_s \sim 7 \text{ ns} \sim T_n$ was selected to effectively prevent transitions between different n states avoiding additional line broadening.

The echo is monitored by applying a probe half-cycle pulse (HCP) of duration $T_p \sim 0.6 \text{ ns}$ and amplitude sufficient to ionize $\sim 50\%$ of the atoms, along the z axis after a variable time delay τ_{delay} and measuring the overall sur-

vival probability (after the dc field has returned to zero) using field ionization [19]. Because the probe HCP is very short, $T_p \ll T_n$, it simply delivers an impulse or kick Δp_p to the electron resulting in an energy transfer $\Delta E = p_z \Delta p_p + (\Delta p_p)^2/2$. As ΔE is a function of p_z , the survival probability reflects the time evolution of the average value $\langle p_z \rangle$ of the wave packet. Because of the cylindrical symmetry, the measurements are insensitive to rotational motion about the z axis and equivalent to probing motion in the rotating frame. The survival probability maps out the variation of the orientation and elongation of the Kepler ellipse [Fig. 2(a)]—the “Stark beats” of the electric dipole moment.

Figure 3 shows that without field reversal the amplitude of the Stark beats decreases steadily with time due to dephasing. Reversal of the field leads to the appearance of a strong echo. Figure 3 includes results of classical trajectory Monte Carlo (CTMC) simulations. The (restricted) microcanonical ensemble of points in phase space that represents the initial mix of Stark states [18], which is centered on $nA_x = 292$, is propagated in time according to Hamilton’s equation of motion. This initial state with a narrow distribution of $k(=nA_z)$ centered on $k = 0$ is chosen to suppress the quadratic frequency shift $\omega_k^{(2)}$. The simulations mirror the behavior seen experimentally. Small differences can be attributed to uncertainties in the size of the applied field F and the exact mix and orientation of the initial states. The relative size of the echo is smaller than calculated providing evidence of decoherence associated with irreversible dephasing. This may be caused by external perturbations introduced, for example, by fluctuating external fields (noise), radiation fields, or collisions with background gas.

The dephasing and subsequent rephasing of the wave packet can be seen clearly in the time evolution of the probability density of the pseudospins displayed in Fig. 4 in the ($J_+^{x'}$, $J_+^{y'}$) plane. The precessional motion proceeds around the circle denoted by the dashed line with angular

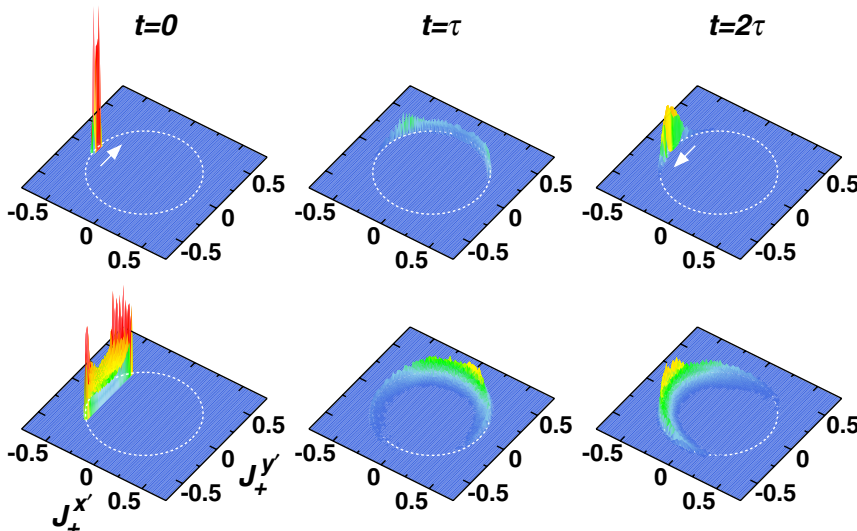


FIG. 4 (color online). Time evolution of the probability density in the ($J_+^{x'}$, $J_+^{y'}$) plane. The snapshots are taken at $t = 0$, τ , and 2τ , where $\tau = 500 \text{ ns}$. Upper panels: evolution for initial state with maximal transverse polarization (see text). Lower panels: evolution for the state realized in the experiment (see text). The arrows denote the precessional motion of the wave packet. $J_+^{x'}$ and $J_+^{y'}$ are expressed in scaled units.

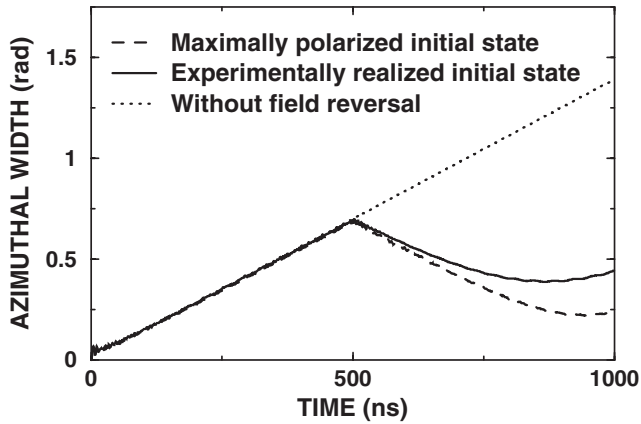


FIG. 5. CTMC simulations of the width $\Delta\phi_+(t)$ of the wave packet in the azimuthal angle, ϕ_+ . The initial linear diffusion $\Delta\phi_+ \propto t$ is reversed at $t = \tau = 500$ ns due to field reversal. Results are included for three different cases: the maximally polarized initial state (dashed line), the experimentally realized initial state (solid line), and without field reversal (dotted line). The magnitude of the field is 20 mV/cm. To compare only the diffusive nature of $\Delta\phi_+$, the initial spread is subtracted from the results.

velocity $\omega_k(F)$. The sense of rotation is reversed after the field is reversed. The upper frames in Fig. 3 are for an initial state maximally polarized in the transverse plane (a superposition of extreme parabolic states $nA_x = n - 1$ along the x axis, i.e., $k \sim 0$, with $342 < n < 358$). The lower frames correspond to an initial state that mimics the experimental initial state. The probability densities are initially strongly localized in azimuthal angle $\phi_+ = \tan^{-1}(J'_+/J'_+)$ and centered near $\phi_+ = \pi$. They evolve around the circle as $\phi_+ = \pi + \omega_k(F)t$ and spread as they dephase. After field reversal at $t = \tau$ the wave packets rephase leading to an echo at $t = 2\tau$. The echo is nearly ideal for the maximally polarized state but is less well defined for the experimental state because the initial k distribution is broader. The spreading and rephasing behavior can be quantified using the width $\Delta\phi_+$ of the distribution in the azimuthal angle ϕ_+ (Fig. 5). Initially, the angular diffusion is linear, $\Delta\phi_+ \propto t$, but is reversed upon reversal of the field. The value of the width at the time of the echo can be used to accurately determine the degree of irreversible dephasing or decoherence.

Several applications of the electric dipole echo demonstrated in the present work can be envisioned. Prime among them is the exploration of decoherence. Unlike revivals, the echo allows decoherence to be probed over a wide range of decoherence times as the time of field reversal can be varied. Moreover, the response to “colored” noise [20] can be explored in a controlled fashion. Another possible extension is the controlled modulation of the dipole blockade in a Rydberg gas starting with an ultracold

gas in an optical lattice [10,21]. The time-dependent (quasi-permanent) electric dipole of the Stark Rydberg wave packet induces long-range interactions with nearby atoms that should dominate over induced dipole-dipole interactions.

This research is supported by the FWF-SFB-F016 (Austria), OBES, US DOE to ORNL managed by the UT-Batelle LLC under Contract No. DE-AC05-00OR22725, the NSF (No. PHY-0353424), and the Robert A. Welch Foundation.

- [1] E. L. Hahn, Phys. Rev. **80**, 580 (1950).
- [2] C. P. Slichter, *Principles of Magnetic Resonance* (Springer, New York, 1992).
- [3] J. Emerson, Y. S. Weinstein, M. Saraceno, S. Lloyd, and D. G. Cory, Science **302**, 2098 (2003).
- [4] N. A. Gershenfeld and I. L. Chuang, Science **275**, 350 (1997).
- [5] I. D. Abella, N. A. Kurnit, and S. R. Hartmann, Phys. Rev. **141**, 391 (1966).
- [6] A. L. Alexander, J. J. Longdell, M. J. Sellars, and N. B. Manson, Phys. Rev. Lett. **96**, 043602 (2006).
- [7] R. A. Jalabert and H. M. Pastawski, Phys. Rev. Lett. **86**, 2490 (2001).
- [8] D. Jaksch, J. I. Cirac, P. Zoller, S. L. Rolston, R. Côté, and M. D. Lukin, Phys. Rev. Lett. **85**, 2208 (2000).
- [9] J. Ahn, T. C. Weinacht, and P. H. Bucksbaum, Science **287**, 463 (2000).
- [10] M. D. Lukin, M. Fleischhauer, R. Cote, L. M. Duan, D. Jaksch, J. I. Cirac, and P. Zoller, Phys. Rev. Lett. **87**, 037901 (2001).
- [11] R. S. Minns, M. R. Kutteruf, H. Zaidi, L. Ko, and R. R. Jones, Phys. Rev. Lett. **97**, 040504 (2006);
- [12] H. Maeda, D. V. L. Norum, and T. F. Gallagher, Science **307**, 1757 (2005).
- [13] C. J. Myatt, B. E. King, Q. A. Turchette, C. A. Sackett, D. Kielpinski, W. M. Itano, C. Monroe, and D. J. Wineland, Nature (London) **403**, 269 (2000).
- [14] H. Wen, S. N. Pisharody, J. M. Murray, and P. H. Bucksbaum, Phys. Rev. A **71**, 013407 (2005).
- [15] L. D. Landau and E. M. Lifshitz, *Mechanics* (Pergamon, Oxford, 1960).
- [16] I. C. Percival and D. Richards, J. Phys. B **12**, 2051 (1979).
- [17] A. Sommerfeld, *Atombau und Spektrallinien* (Harri Deutsch, Frankfurt, 1978).
- [18] F. B. Dunning, J. C. Lancaster, C. O. Reinhold, S. Yoshida, and J. Burgdörfer, Adv. At. Mol. Opt. Phys. **52**, 49 (2005).
- [19] W. Zhao, J. J. Mestayer, J. C. Lancaster, F. B. Dunning, C. O. Reinhold, S. Yoshida, and J. Burgdörfer, Phys. Rev. Lett. **95**, 163007 (2005).
- [20] S. Yoshida, C. O. Reinhold, J. Burgdorfer, W. Zhao, J. J. Mestayer, J. C. Lancaster, and F. B. Dunning, Phys. Rev. A **75**, 013414 (2007).
- [21] C. Ates, T. Pohl, T. Pattard, and J. M. Rost, Phys. Rev. Lett. **98**, 023002 (2007).